Biomaterials 33 (2012) 3013–3024

Contents lists available at SciVerse ScienceDirect

Biomaterials

journal homepage: www.elsevier.com/locate/biomaterials

Magnetite-loaded fluorine-containing polymeric micelles for magnetic resonance imaging and drug delivery

Xiaolong Li [a,1], Huan Li [b,1], Guoqiang Liu [a], Ziwei Deng [a], Shuilin Wu [a,c], Penghui Li [c], Zushun Xu [a,c,***], Haibo Xu [b,**], Paul K. Chu [c,*]

[a] Ministry of Education Key Laboratory for the Green Preparation and Application of Functional Materials, Hubei University, Wuhan, Hubei 430062, China
[b] Radiology Department of Union Hospital, Tongji Medical College of Huazhong University of Science and Technology, Wuhan, Hubei 430030, China
[c] Department of Physics & Materials Science, City University of Hong Kong, Tat Chee Avenue, Kowloon, Hong Kong, China

ARTICLE INFO

Article history:
Received 9 December 2011
Accepted 23 December 2011
Available online 13 January 2012

Keywords:
Copolymers
Fluorine-fluoride
Micelle
MRI
Drug delivery

ABSTRACT

Magnetite (Fe_3O_4) – loaded polymer micelles (denoted as "magnetomicelles") are produced by self-assembly of fluorine-containing amphiphilic poly(HFMA-*g*-PEGMA) copolymers with oleic acid modified Fe_3O_4 nanoparticles in an aqueous medium. The oleic acid modified Fe_3O_4 nanoparticles form small clusters in the poly(HFMA-*g*-PEGMA) micelles with a mean diameter of 100 nm and the magnetomicelles show high stability in an aqueous medium due to the high hydrophobic fluorine segments in graft copolymers enhance the stability of the micelles. The magnetomicelles also show good cytocompatibility based on the MTT cytotoxicity assay and possess paramagnetic properties with saturation magnetization of 17.14 emu/g.Their good stability, cytocompatibility, and paramagnetic properties render the materials attractive in drug delivery and *in vivo* magnetic resonance imaging (MRI) applications. Controlled release of hydrophobic drug-5-fluorouracil is achieved from the magnetomicelles with a loading efficiency of 20.94 wt%. The magnetomicelles have transverse relaxivity rates (r_2) of 134.27 mM^{-1} s^{-1} and exhibit high efficacy as a negative MRI agent in T_2-weighted imaging. *In vivo* MRI studies demonstrate that the contrast between liver and spleen is enhanced by the magnetomicelles. These favorable properties suggest clinical use as nanocarriers in drug delivery applications and contrast agents in MRI.

1. Introduction

Magnetic nanoparticles (MNPs) play important roles in biotechnology and medicine such as targeted drug delivery [1–3], bimolecular labeling and separation [4,5], as well as magnetic resonance imaging (MRI) [6–8]. As a result of this drive to integrate MNPs into biological system, surface coatings are necessarily applied to improve the colloidal stability, cytocompatibility, and immunogenicity of MNPs and different fabrication techniques such as exchange of surface ligands [9,10], silica coating [11], and encapsulation with amphiphilic molecules including small surfactants [12], lipids [13] and amphiphilic copolymers [14–16] have been reported.

In particular, amphiphilic copolymers are particularly promising due to their unique chain architecture and self-assembling properties. Amphiphilic copolymers consisting of both hydrophobic and hydrophilic segments can self-assemble into superamolecular hydrophobic core - hydrophilic shell structures in aqueous media [17,18]. The hydrophobic micelle core provides an ideal nano-scale compartment for hydrophobic nanoparticles and the hydrophilic shell forms a steric barrier to preclude aggregation in an aqueous medium [19,20]. As a result, these polymeric micelles can be used as nanocarriers of hydrophobic nanoparticles for MRI contrast agents to achieve longer blood half-life and better contrast. In addition to diagnostic imaging applications, amphiphilic copolymers have received increasing attention in loading hydrophobic drugs such as paclitaxel and doxorubicin in drug delivery applications [21,22]. As a result, many efforts have been made to encapsulate magnetic nanoparticles with amphiphilic block copolymers such as polyester-based amphiphilic block copolymers [15,23,24] or block copolymers obtained from controlled radical polymerization (ATRP and RAFT methods) [25–27]. As another kind of amphiphilic copolymers, graft copolymers can be prepared by common synthetic methods and they not only form polymeric micelles with

* Corresponding author. Tel.: +86 852 34427724; fax: +86 852 34420542.
** Corresponding author. Tel.: + 86 27 85726410; fax: + 86 27 85726919.
*** Corresponding author. Ministry of Education Key Laboratory for the Green Preparation and Application of Functional Materials, Hubei University, Wuhan, Hubei 430062, China. Tel.: +86 27 88661879; fax: +86 27 88665610.
E-mail addresses: zushun25@yahoo.com.cn (Z. Xu), xuhaibo1120@hotmail.com (H. Xu), paul.chu@cityu.edu.hk (P.K. Chu).
[1] These two authors contributed equally to this project.

0142-9612/$ – see front matter © 2011 Elsevier Ltd. All rights reserved.
doi:10.1016/j.biomaterials.2011.12.042

less chains, but also prevent the polymer chains from sliding away in an aqueous solution [28,29]. Therefore, magnetic nanoparticles encapsulated by graft copolymers may produce stable magnetomicelles suitable for drug delivery and MRI applications [30,31].

In spite of the aforementioned potential, there are risks associated with the use of graft amphiphilic copolymers under biological conditions because the weak hydrophobic force resulting from the hydrophobic chains can rupture the micelles [32]. Therefore, development of reliable amphiphilic graft copolymers for encapsulation of magnetic nanoparticles is of great importance. It has been reported that amphiphilic copolymers with the fluorocarbon-hydrocarbon structure have the strong tendency to self-aggregate into stable well-organized micelles [33,34] due to the unique characteristics inherent to fluoropolymers such as high hydrophobicity, good thermal stability, and low surface energy [35,36]. The strong hydrophobic interactions and high fluidity of the fluorine-containing polymers are supposed to have strong interaction with hydrophobic nanoparticles and keep magnetomicelles stable in the circulation.

In this work, stable magnetomicelles are produced by self-assembly of fluorine-containing amphiphilic poly(HFMA-g-PEGMA) copolymers with oleic acid modified Fe_3O_4 nanoparticles in an aqueous medium. The fluorocarbon segments form a stable hydrophobic core to adsorb oil-based nanoparticles, and the PEGMA segments enhance the solubility in water thus reducing the cytotoxicity of the hybrid micelles. To assess the suitability of these magnetomicelles as a drug carrier, drug loading and *in vitro* release studies are performed using 5-fluorouracil (5-FU) as a hydrophobic model drug. To evaluate the feasibility of these magnetomicelles as MRI contrast agents, the MRI contrast is monitored *in vivo*.

2. Materials and methods

2.1. Materials

2, 2, 3, 4, 4, 4-hexafluorobutyl methacrylate (HFMA) purchased from Xeogia Fluorine–Silicon Chemical Company (Harbin, China, Chemical Purity) was distilled at reduced pressure before use. Methoxy poly (ethylene glycol) monomethacrylate (PEGMA) (average Mn 950 g/mol) was obtained from Aldrich and used without further purification. 2, 2′-azobisisobutyronitrile (AIBN, analytical grade) was purified by recrystallization in ethanol. Iron (III) chloride hexahydrate ($FeCl_3 \cdot 6H_2O$), iron (II) chloride tetrahydrate ($FeCl_2 \cdot 4H_2O$), oleic acid (OA), ammonium hydroxide solution ($NH_3 \cdot H_2O$, 36%), ethanol, hexane, and tetrahydrofuran (THF) were purchased from Sinopharm Chemical Reagent Co. Ltd., China and 5-fluorouacil and 3-(4, 5-dimethyl thiazol-2-yl)-2, 5-diphenyl tetrazolium bromide (MTT) were purchased from Sigma-Aldrich.

2.2. Synthesis of amphiphilic poly (HFMA-g-PEGMA) copolymers

The amphiphilic poly (HFMA-g-PEGMA) copolymers were synthesized by free radical polymerization [37,38]. In a typical reaction, the solution consisting of the PEGMA macromonomer (1.023 g), HFMA (0.787 g), AIBN (0.085 g), and 10 mL of THF was added to a 50 mL round-bottom flask with a magnetic stirrer, deoxygenated under vacuum, and backfilled with nitrogen several times in an ice bath.-Polymerization was conducted for 24 h at 75 °C and the amphiphilic poly (HFMA-g-PEGMA) copolymers were collected by precipitation in hexane. The unreacted monomers were removed using three dissolution-precipitation cycles in THF and hexane, respectively. Finally, the purified products were dried under vacuum at 35 °C for later use.

2.3. Preparation of oleic acid modified Fe_3O_4 nanoparticles

The Fe_3O_4 nanoparticles were prepared by precipitation of Fe (III) and Fe (II) in an alkaline solution [39]. 13.5 g of $FeCl_3 \cdot 6H_2O$ and 6 g of $FeCl_2 \cdot 4H_2O$ were dissolved in 150 mL of distilled water under nitrogen at room temperature and then 40 mL of $NH_3 \cdot H_2O$ was added quickly to the solution under vigorous stirring to produce black precipitates. After heating at 80 °C for 1 h, 6 g of oleic acid was added dropwise at a constant rate and the reaction proceeded for another hour.Afterwards, the mixture was cooled to room temperature, and the oleic acid modified magnetic fluid was collected magnetically and washed by ethanol and hexane several times. The black slurry was further dispersed in hexane for storage.

2.4. Preparation of magnetomicelles

The oleic acid modified Fe_3O_4 nanoparticles (0.310 g) were added to 50 mL of water containing 0.310 g of the amphiphilic poly (HFMA-g-PEGMA) copolymers. It was then mixed manually followed by sonication for 15 min. Afterwards, hexane was evaporated at 70 °C in a water bath under sonication while nitrogen was bubbled to form the magnetomicelles.

2.5. Effects of HFMA/PEGMA ratio on magnetic nanoparticles loading efficiency

To investigate the loading efficiency of the magnetic nanoparticles, a series of poly(HFMA-g-PEGMA) samples with HFMA/PEGMA mass ratios from 0.2:1 to 1.2:1 were synthesized. The oleic acid modified nanoparticles were added to the amphiphilic copolymers with the same ratio as stated in section 2.4. After removal of unencapsulated nanoparticles by filtering, all the samples were lyophilized and the magnetic nanoparticles loading densities were investigated using atomic absorption spectrophotometry (AA-680).Succinctly speaking, the freeze-dried micelles were weighed and added to a 1 M HCl solution to disperse the magnetite nanoparticles.The iron concentration was determined at the specific Fe absorption wavelength (248.3 nm) and the nanoparticles loading density was calculated as the ratio of iron oxide to the total weight of the magnetomicelles.

2.6. In vitro cytotoxicity test

The cytotoxicity of the magnetomicelles was assessed by the MTT assay. HeLa cells were cultured in Dubecco's Eagle Medium supplemental medium with 10% fetal bovine serum and incubated at 37 °C with 5% CO_2. The culture medium was added to a 96-well plate and treated with different concentrations of magnetomicelles (dose diluted by complete medium, 0–250 μg/mL) for 24 h.Afterwards, the medium was removed and 25 μL of the MTT stock solution (5 g/L in PBS) was added to each well to obtain a final concentration of 1 g/L. The cultures were incubated for another 4 h. After discarding the culture medium, DMSO (100 uL/well) was added to dissolve the precipitate and the absorbance at 570 nm was measured from the solution using a Microplate reader. The relative cell viability was calculated by the following equation: Relative cell viability % = ($OD_{treated}/OD_{control}$) x 100, where $OD_{treated}$ was obtained in the presence of magnetomicelles and $OD_{control}$ was obtained in the absence of magnetomicelles.

2.7. 5-FU drug loading into the magnetomicelles

The mixture containing 50 mg of 5-FU drug and 10 mL of the aqueous stock solution prepared in section 2.4 was agitated for 20 min at room temperature. After standing for 1 h, some aggregates in the mixture were removed by a filter (Ø = 0.45 um) and then the 5-FU drug loaded into the magnetomicelles were separated by a magnet and freeze-dried for the subsequent drug release study. The concentration of released 5-FU was determined from the ultraviolet–visible (UV–Vis) spectrum at a wavelength of 265 nm. The drug loading coefficient (DL %) was calculated using the following equation:

$$DL\% = \frac{\text{original drug added(mg)} - \text{drug remained in the supernatant(mg)}}{\text{weight of the feeding polymer(mg)}} \times 100\%. \quad (1)$$

2.8. In vitro drug release study

In vitro drug release from the magnetomicelles was assessed in PBS (pH = 7.4) at 37 °C. 50 mg of the 5-FU-loaded magnetomicelles were dispersed in 10 mL of PBS and placed in a dialysis bag with a molecular weight cut-off of 14000 Da. The dialysis bag was suspended in 100 mL of PBS at a constant temperature and stirred (100 rpm). 1 mL of the released medium was taken out and replaced by 1 mL of fresh PBS periodically. The amount of released 5-FU was determined by UV–vis spectrophotometry at 265 nm.In the control experiment, 10 mg of free 5-FU instead of 5-FU-loaded magnetomicelles were employed to determine the release rate using the same experimental protocols.

2.9. MRI characterization and in vivo MRI

To determine the relaxivity, the magnetomicelles were diluted in distilled water with iron concentrations in the range of 0–0.4192 mmol/L. The samples were transferred to a 96-well plate, placed in an MR scanner, and tested by using a number of MR sequences. The T_2 relaxation time of the suspension was computed using in-house software (MATLAB V7.1).The T_2 relaxation rates were plotted versus iron concentrations and the relaxivity was computed using linear regression analysis (Microsoft EXCEL).

The *in vivo* MRI studies were performed in SD mice weighing approximately 200 g.The mice were anaesthetized by trichloroacetaldehyde hydrate (10%) with a dose of 40 mg/kg body weight at normal body temperature. The mice were scanned before and after administration of 1 mL of the magnetomicelles solution

with a dose of 5 mg (Fe)/kg body weight through the tail vein for 4 h.The coronal and transversal cross sections images were acquired from the MR scanner.The signal intensity (SI) was measured at each time point and the relative SI changes were plotted against time.The relative signal enhancement values (RSEs) were calculated using SI measurements before (SI_{pre}) and after (SI_{post}) injection of the contrast agents by the formula: $[(SI_{post}-SI_{pre})/SI_{pre}] \times 100\%$. The SI_{post} values were collected at time points of 10 min, 1 h, 2 h, 3 h, and 4 h.

All the animals were managed and treated according to the rules and regulations of the Institutional Animal Care and Use Committee at Hubei University, and the animal protocols were also approved by the Institutional Animal Care.

2.10. Histology analysis

The mice were sacrificed 8 h after injection with the magnetomicelles.The liver, spleen, kidney, and lung of the mice were fixed in 4% paraformaldehyde for 24 h and transferred to 30% sucrose in the PBS buffer. The tissues were prepared for histological analysis by Prussian blue staining and neutral red solution counterstaining.

2.11. Characterization

The structure of the amphiphilic poly (HFMA-*g*-PEGMA) copolymers, oleic acid modified Fe_3O_4 nanoparticles, and magnetomicelles was determined by Fourier Transfer infrared (FTIR, PerkinElmer Spectrum One, USA). The samples were compressed into KBr pellets and the spectra were taken from 4000 to 500 cm^{-1}.

^1H NMR and ^{19}F NMR were used to confirm the chemical structure of the amphiphilic poly (HFMA-*g*-PEGMA) copolymers.The NMR experiments were conducted on the UNITY INVOA 600MHz spectrometer (Varian, USA) with $CDCl_3$ as the solvent.

A Krüss interface tension meter (KrüssGmbH, Hamburg, Germany) was used to measure the surface tension of the amphiphilic poly (HFMA-*g*-PEGMA) copolymers using the pendant drop method at 25 °C. Amphiphilic poly (HFMA-*g*-PEGMA) copolymers with different concentrations were prepared in distilled water for the surface tension measurement and the critical micelle concentration was determined.

The molecular weight and molecular weight distribution of the amphiphilic poly (HFMA-*g*-PEGMA) copolymers were determined on the Waters 2414 gel permeation choromatograph using a series of monodispersed polystyrenes as the calibration standard and THF as the eluent using a flow rate of 1.0 mL/min at 35 °C.

The morphology of the nanoparticles (oleic acid modified Fe_3O_4 nanoparticles and magnetomicelles) was examined by transmission electron microscopy (TEM, Tecnai G20, FEI Corp. USA). The nanoparticles for the TEM analysis were prepared by drying the dispersion on amorphous carbon coated copper grids.

The dynamic size and size distribution of the nanoparticles were characterized by dynamic light scattering (DLS) (Autosize Loc-Fc-963, Malven Instrument). The crystallographic structure of the magnetic and composite particle powders was determined by X-ray diffractometry (XRD, D/MAX-IIIC, Japan). The diffraction (XRD) patterns were taken from 20 to 90 ° (2θ) using Cu K_α radiation at a scanning rate of 15°/min.

The thermogravimetric analysis was performed on the PerkinElmer TGA-7. The dried powder samples were heated at the rate of 10 °C/min in a nitrogen atmosphere from room temperature to 600 °C.

The magnetic properties of the oleic acid modified Fe_3O_4 nanoparticles and magnetomicelles were measured on a vibrating-sample magnetometer (VSM, HH-15, China) at 298 K under an applied magnetic field. The UV–visible absorption spectra were obtained from the released 5-FU (Hitachi UV-3000, Japan) at room temperature.

The MRI experiments were performed *in vitro* and *in vivo* at 25 °C using a 3.0 Tesla whole-body MR scanner (MAGNETOM Trio, A Tim System 3T, Siemens, Munich, Germany) in combination with an 8-channel wrist joint coil.The following parameters were used in the measurement of the magnetomicelles transverse relaxivity: field of view (FOV) = 120 mm, base resolution = 384 × 384, slice thickness = 1.5 mm, multiple echo times (TE) = 20, 40, 60, 80, 100, 120, or140 ms, repetition time (TR) = 2000 ms, and scanning time = 13–14 min. In the *in vivo* imaging studies, the scanning parameters were as follows: field of view (FOV) = 100 mm, slice thickness = 2.0 mm, multiple echo times (TE) = 62 ms, repetition time (TR) = 3000 ms, and flip angle = 120 °.

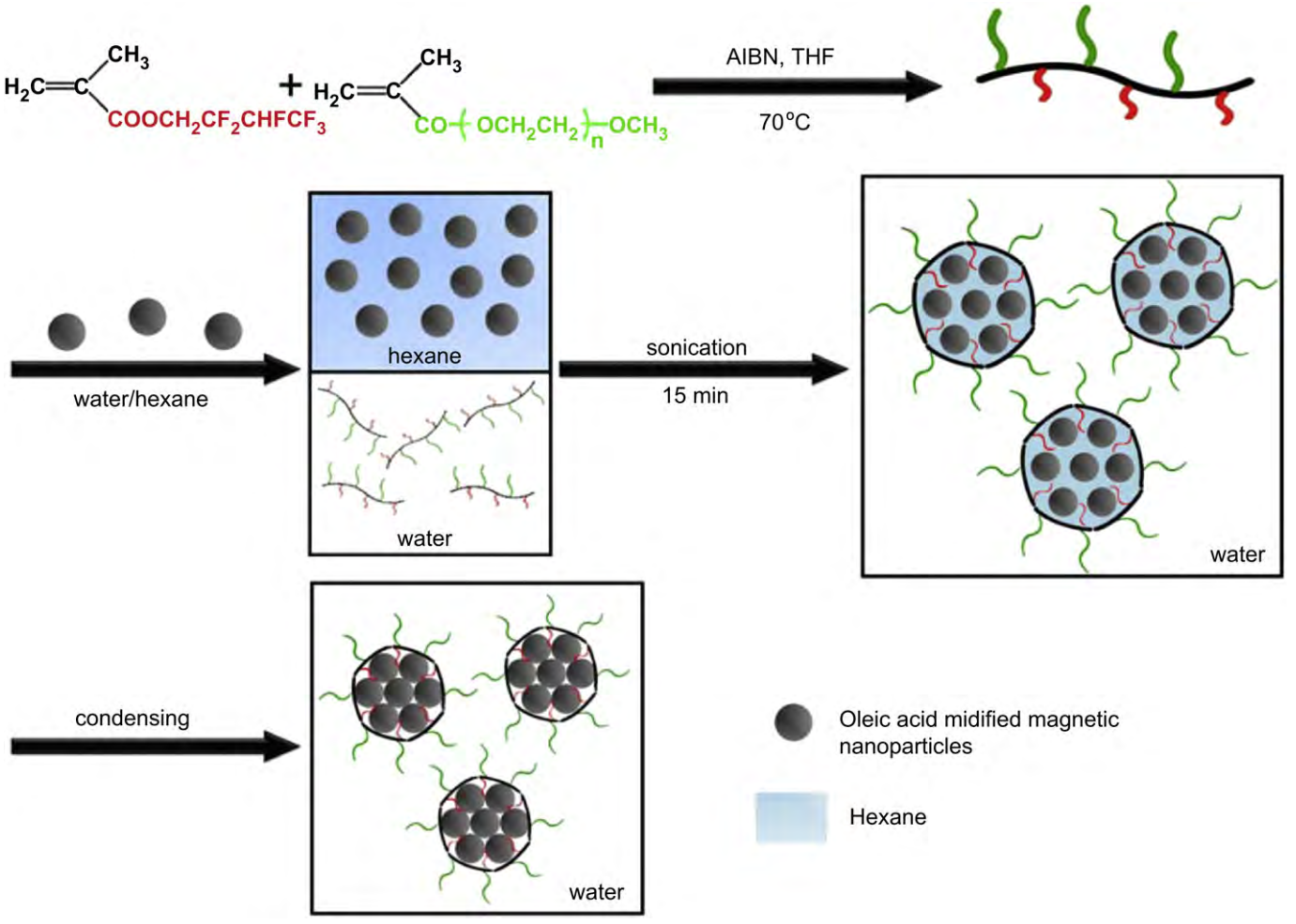

Scheme 1. Schematic illustration of the formation of magnetomicelles during the assembly process of the fluorine-containing amphiphilic poly (HFMA-g-PEGMA) copolymers and oleic acid modified Fe_3O_4 nanoparticles in an aqueous medium.

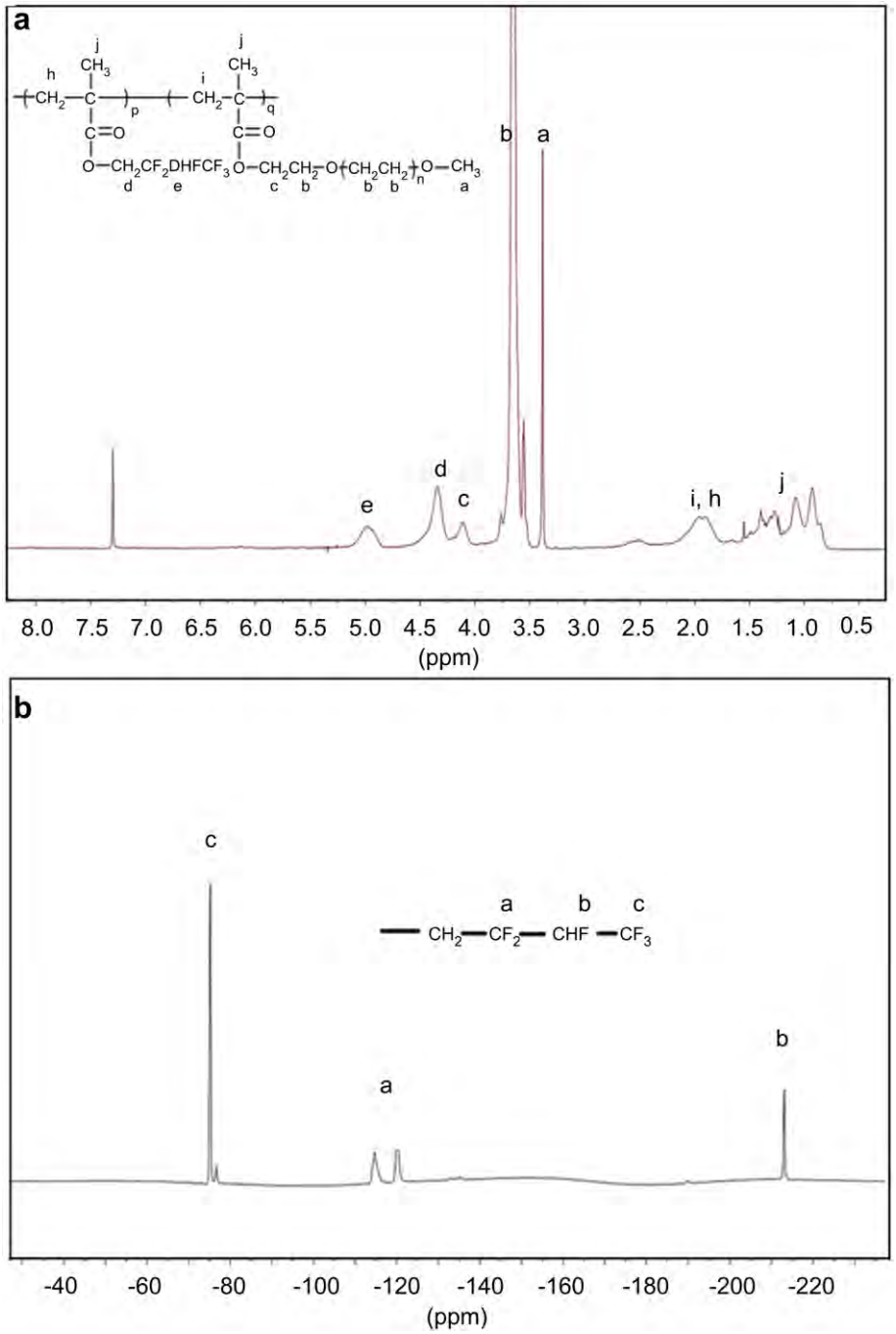

Fig. 1. (a) ^{1}H NMR and (b) ^{19}F NMR spectra of the fluorine-containing amphiphilic poly (HFMA-g-PEGMA) copolymers.

3. Results and discussion

The experimental design is illustrated in Scheme 1. Amphiphilic poly(HFMA-g-PEGMA) copolymers synthesized by polymerization of hydrophobic HFMA monomers and hydrophilic MPEGMA macromonomers in THF at 70 °C are used as an emulsifier to assemble the oleic acid modified Fe_3O_4 nanoparticles in water. In the assembly process, the oleic acid modified Fe_3O_4 nanoparticles dispersed in hexane are mixed with the amphiphilic poly(HFMA-g-PEGMA) copolymers to form two immiscible liquids under sonication. The oil phase consisting of the oleic acid modified Fe_3O_4 nanoparticles coexist inside the polymer micelles through emulsification of the amphiphilic poly(HFMA-g-PEGMA) copolymers. After evaporation of hexane, the Fe_3O_4 nanoparticles in the primary oil droplets condense to form stable Fe_3O_4 clusters with protection provided by the polymer micelles which are used as magnetomicelles in our subsequent drug delivery and *in vivo* MRI experiments.

3.1. Characterization of amphiphilic poly(HFMA-g-PEGMA) copolymers

As a type of macro-emulsifier, the amphiphilic poly(HFMA-g-PEGMA) copolymers are synthesized by polymerization in THF using AIBN as the initiator. The structure of the amphiphilic

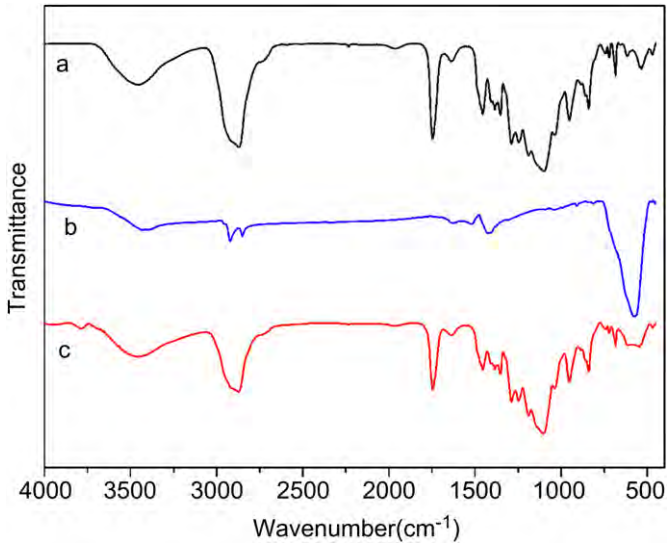

Fig. 2. FTIR spectra of (a) amphiphilic poly(HFMA-g-PEGMA) copolymer, (b) oleic acid modified Fe_3O_4 nanoparticles, and (c) magnetomicelles.

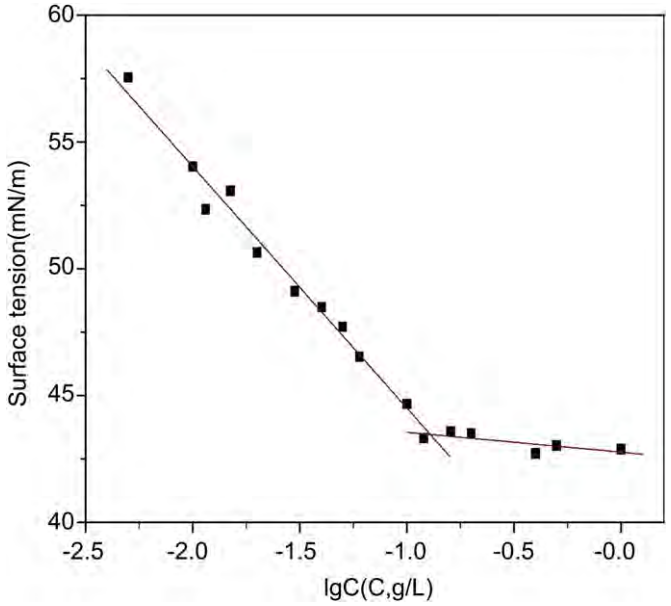

Fig. 3. Critical micelle concentrations of poly(HFMA-g-PEGMA) determined by surface tension measurements.

poly(HFMA-g-PEGMA) copolymers is determined by ^{1}H- NMR, ^{19}F-NMR, and FTIR. The ^{1}H NMR spectra in Fig. 1a reveal prominent chemical shifts. The broad peaks at δ 3.65 ppm (b) ($-OCH_2CH_2-$), δ 3.38 ppm (a) (terminal H of PEGMA $-OCH_3$), and δ 4.12 ppm(c) ($COOCH_2-$) belong to the repeating units of the PEG segment. The peaks at δ 4.35 ppm (d) ($-OCH_2.CF_2$) and δ 4.99 ppm (e) ($CF_2-CHF-CF_3$) correspond to the repeating unit of the HFMA segment. The signals from the terminal methyl group protons and methylene protons of the copolymer backbone can be observed at approximately 0.92–1.5 ppm (j) and 1.93 ppm (i, h), respectively. To further characterize the poly(HFMA-g-PEGMA) , ^{19}F NMR is conducted to determine the fluorocarbon moiety in the copolymers. The ^{19}F NMR spectrum of the copolymers in Fig. 1b confirms the presence of three types of fluorine resonances originating from the HFMA segments. The shift at −75.16 ppm (c) is assigned to the end $-CF_3$ group and shift at −213.05 ppm (b) to the −CHF group. The peak of $-CH_2-CF_2-$ splits into two peaks at −114.58 ppm and −120.12 ppm (a) due to influence by the $-OCH_2-CF_2$ group.

FTIR spectra are acquired from the amphiphilic poly(HFMA-g-PEGMA) copolymers (Fig. 2a). The absorption peaks at 1000–1200 cm^{-1} are wider and flatter than those of the copolymers without fluorocarbon bonds. The characteristic peak of C-F appears at 1388 cm^{-1} because of the HFMA segment. The peak at 1740 cm^{-1} can be attributed to the CO characteristic stretching adsorption of both HFMA and PEGMA.The results indicate that amphiphilic poly (HFMA-g-PEGMA) copolymers have been synthesized by free radical polymerization.

To evaluate the surface properties of the amphiphilic poly (HFMA-g-PEGMA) copolymers in an aqueous medium, the critical micelle concentration (CMC) of the amphiphilic poly (HFMA-g-PEGMA) copolymers is evaluated by surface tension measurements. Usually, the amphiphilic copolymer concentration is above CMC and these polymeric micelles are formed to minimize the interfacial energy. Theoretically, the interfacial tension show exhibit a sudden change at or near CMC [40], and so the surface tension measurements should be carried out over a wide range of concentrations. Fig. 3 shows that the surface intension decreases linearly with the logarithmic copolymer concentrations at low concentrations but is flat in the crossover region. The CMC determined from the intersection point of those two straight lines is about 0.129 mg/mL.

The molecular weight and molecular weight distribution of the PEGMA monomer and poly (HFMA-g-PEGMA) copolymer are determined by GPC.The chromatograms acquired from the PEGMA monomer and poly (HFMA-g-PEGMA) copolymers are shown in Fig. 4. The chromatogram of a typical poly (HFMA-g-PEGMA) copolymer indicates a unimodal molecular weight and successful polymerization.

3.2. Characterization of magnetomicelles

The oleic acid modified Fe_3O_4 nanoparticles are examined by TEM and as shown in Fig. 5a, the size of the oleic acid modified

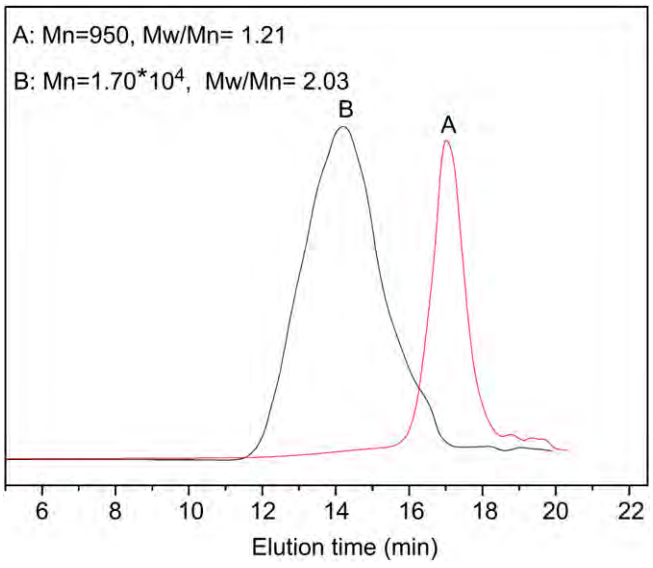

Fig. 4. Typical GPC curves: (A) PEGMA, Mn = 950 g/mol and (B) poly (HFMA-g-PEGMA) (monomer feed ratio HFMA : PEGMA = 0.787 g : 1.023 g), Mn = 1.70 × 10^4 g/mol.

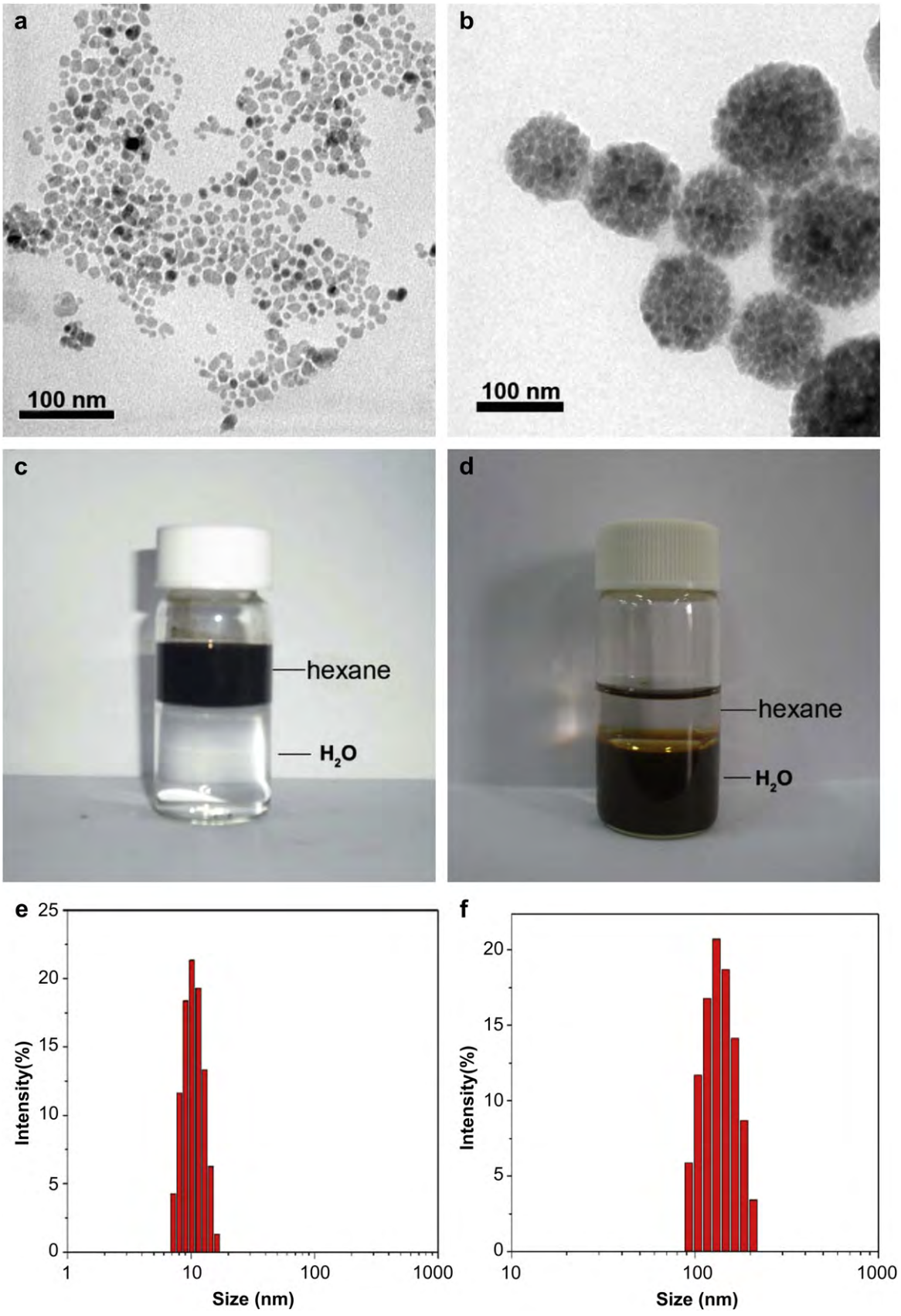

Fig. 5. TEM images of (a) oleic acid modified Fe_3O_4 nanoparticles in hexane and (b) magnetomicelles. Solubility tests of (c) oleic acid modified Fe_3O_4 nanoparticles in hexane and water and (d) magnetomicelles in hexane and water. Size distribution of (e) oleic acid modified Fe_3O_4 nanoparticles in hexane and (f) magnetomicelles in water.

Fe_3O_4 nanoparticles is about 10 nm. They are well dispersed in hexane because of the hydrophobic nature after oleic acid modification (Fig. 5c). The size of the oleic acid modified Fe_3O_4 nanoparticles determined by dynamic light scattering is 10.2 ± 3.2 nm (Fig. 5e) which is the same as that determined from the TEM image (Fig. 5a). The oleic acid modified Fe_3O_4 nanoparticles are further studied by FTIR and XRD. The FTIR peak at 578 cm^{-1} corresponds to Fe-O vibration in Fe_3O_4 and the oleic acid characteristic peaks at 2920 cm^{-1} (ν_{as}–CH_2), 2850 cm^{-1} (ν_s–CH_2), and 1420 cm^{-1} (ν_s–COO^-)(Fig. 2b) confirm that oleic acid has modified the Fe_3O_4 nanoparticles.As shown in the XRD pattern obtained from the oleic acid modified Fe_3O_4 nanoparticles in Fig. 6, the main peaks at 2θ of 30°, 35°, 43°, 57°, 62°, and 74° correspond to the (220), (311), (400), (511), (440), and (533) phases of the face-centered cubic(fcc) Fe_3O_4 crystal structure.

The morphology of the magnetomicelles observed by TEM is also shown in Fig. 5b. The composite micelles with a spherical shape consist of Fe_3O_4 clusters. These Fe_3O_4 clusters in the micelles illustrate magnetite nanoparticles can be packed to a high density in the amphiphilic graft polymers to form magnetomicelles. It should be pointed out that the structure of magnetomicelles reported here is much more closely packed with a density higher than those reported previously on nanoparticles encapsulated by amphiphilic block copolymers [23,41]. The improvement can be ascribed to that the fluorine-containing segments have a strong tendency to adsorb hydrophobic nanoparticles and self-assemble to form the composite micelles.

In our experiments, the oleic acid modified Fe_3O_4 nanoparticles with a hydrophobic nature are well dispersed in hexane but flocculated from the suspension as water is added (Fig. 5c). When the amphiphilic poly (HFMA-*g*-PEGMA) copolymers are in an aqueous medium, water is a poor solvent for both the hydrophobic fluorocarbon domains and hydrophobic nanoparticles thereby inducing micelles formation around the Fe_3O_4 nanoparticles. Therefore, the hydrophobic Fe_3O_4 nanoparticles can be transferred into an aqueous phase with high stability (Fig. 5d) and the high hydrophilicity originates from surface protection provided by the amphiphilic polymers. The average hydrodynamic particle size of the magnetomicelles is 138 nm with a polydispersity index of 0.145 (Fig. 5f), which is larger than that of 100 nm as determined by TEM. It is believed to arise from the aqueous state of the DLS.

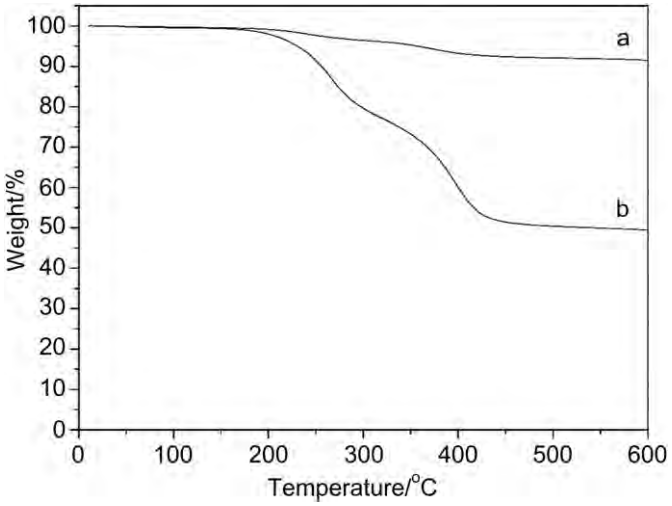

Fig. 7. TGA curves of (a) oleic acid modified Fe_3O_4 nanoparticles and (b) magnetomicelles.

Compared to the FTIR result of the oleic acid modified Fe_3O_4 nanoparticles (Fig. 2b), a broader peak at 614–494 cm^{-1} is observed from the magnetomicelles in Fig. 2c, demonstrating that the amphiphilic poly (HFMA-*g*-PEGMA) copolymers encapsulate the Fe_3O_4 clusters.

Fig. 7 shows the TGA thermograms obtained from the oleic acid modified nanoparticles and Fe_3O_4 clusters encapsulated by the amphiphilic polymers. The magnetic nanoparticles after each stage of modification exhibit distinctive TGA curves related to the relative composition of the magnetomicelles. As shown in Fig. 7a, the 8.5% weight loss in the range of 200–400 °C can be attributed to degradation of oleic acid on the Fe_3O_4 nanoparticles. The first stage of weight loss from 157 to 295 °C corresponds to the degradation of oleic acid and poly (HFMA) whereas the second step at 370–430 °C stems from the decomposition of poly (PEGMA) on the surface of the Fe_3O_4 clusters (Fig. 7b).The Fe_3O_4 content in the magnetomicelles is calculated to be about 49.5 wt% based on the TGA results.

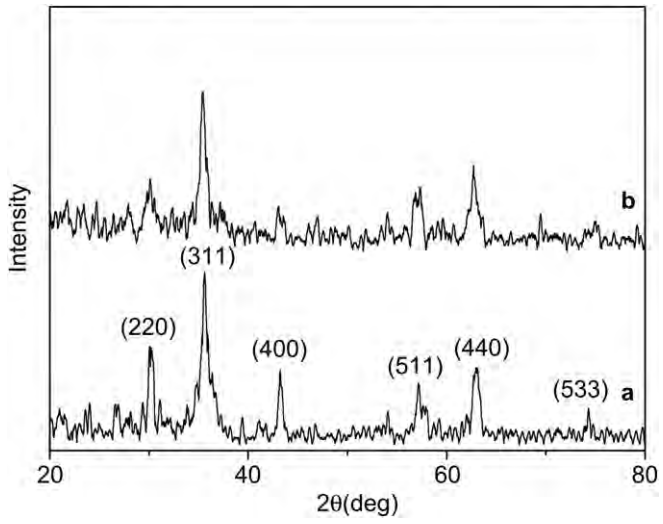

Fig. 6. X-ray powder diffraction patterns of (a) oleic acid modified Fe_3O_4 nanoparticles and (b) magnetomicelles.

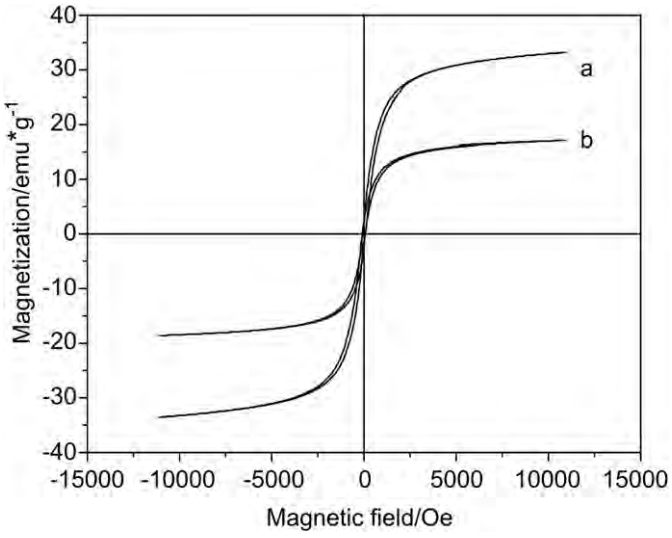

Fig. 8. Magnetic hysteresis loops of (a) oleic acid modified Fe_3O_4 nanoparticles and (b) magnetomicelles.

Table 1
Magnetite nanoparticles loading efficiency of different types of poly(HFMA-g-PEGMA) copolymers.

Sample code	HFMA(g)	PEGMA(g)	Wt% PFMA	Nanoparticles loading (wt. %)
1	0.204	1.012	16.8	21.92
2	0.396	1.005	28.3	35.53
3	0.598	1.000	37.4	40.16
4	0.787	1.013	43.8	49.50
5	1.009	1.017	49.8	36.72
6	1.203	1.016	54.2	31.31

The magnetic hysteresis loops determined from the oleic acid modified Fe_3O_4 nanoparticles and magnetomicelles are displayed in Fig. 8. The saturation magnetization values of the oleic acid modified Fe_3O_4 nanoparticles and magnetomicelles are 33.54 emu/g and 17.14 emu/g, respectively. The loss of magnetization is due to the presence of amphiphilic copolymers. The ratio of coercivity to negligible remnant magnetization (M_r/M_s) of 2.6% reveals magnetomicelles with paramagnetic behavior.

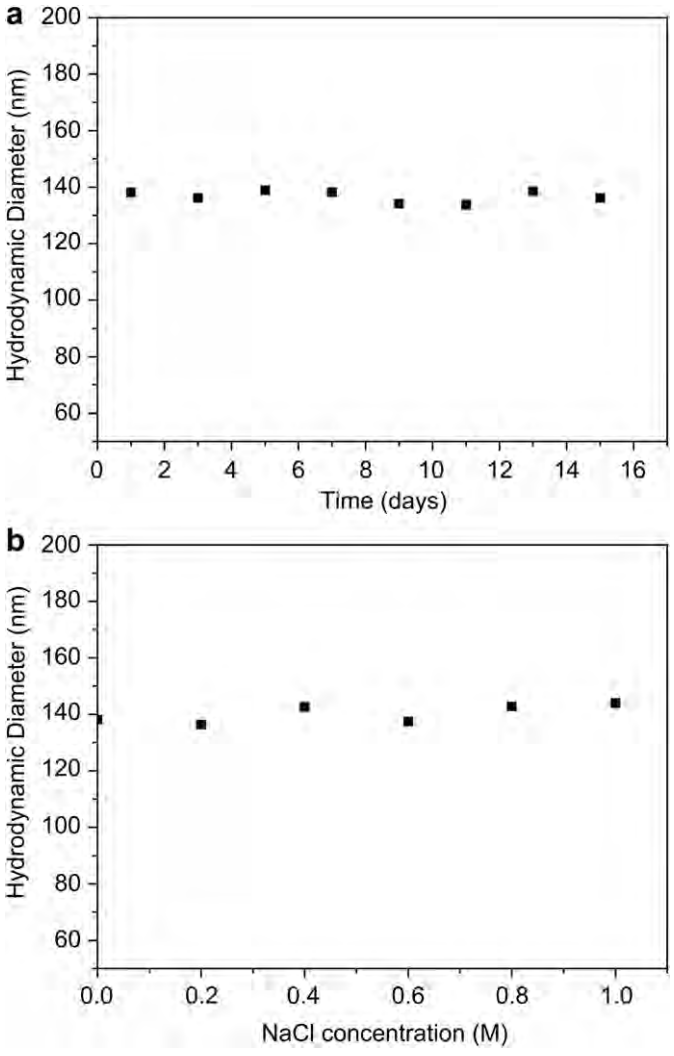

Fig. 9. (a) Storage stability of magnetomicelles in water; (b) Hydrodynamic diameters of magnetomicelles in sodium chloride with different concentrations.

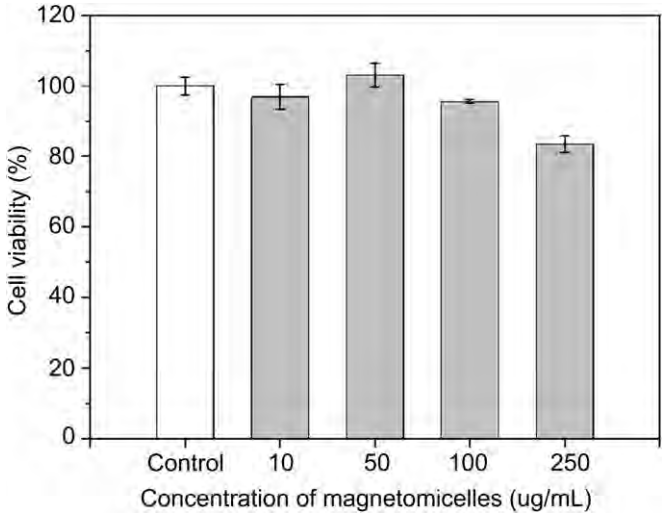

Fig. 10. Cell viability of HeLa cells treated with different concentrations of magnetomicelles for 24 h.

3.3. Effects of HFMA/PEGMA ratio on magnetic nanoparticles loading efficiency

Table 1 shows the poly(HFMA-g-PEGMA) samples with different HFMA/PEGMA mass ratios and magnetite nanoparticles loading efficiency of these different types of poly [(HFMA)x-g-PEGMA].A larger content of the HFMA segment increases the loading capacity up to a maximum value of 49.5 wt% and the polymer/nanoparticles hydrophobic interaction increases as the length of HFMA segment increases. However, beyond this point, the loading capacity decreases with more HFMA segments in the copolymers. This may be due to the increase in the aggregation number per micelles. The total number of micelles in the solution decreases the unit mass of the polymer and consequently the nanoparticle loading capacity. The experimental results are in good agreement with those previously reported [32].

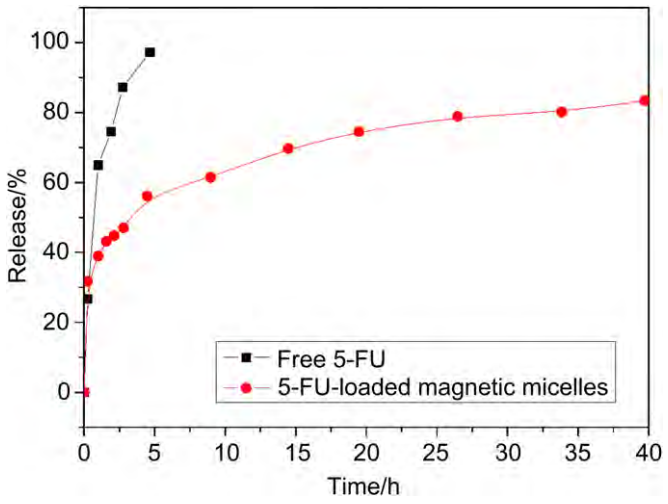

Fig. 11. Release profiles of free 5-FU and 5-FU-loaded magnetomicelles in PBS (pH = 7.4) at 37 °C.

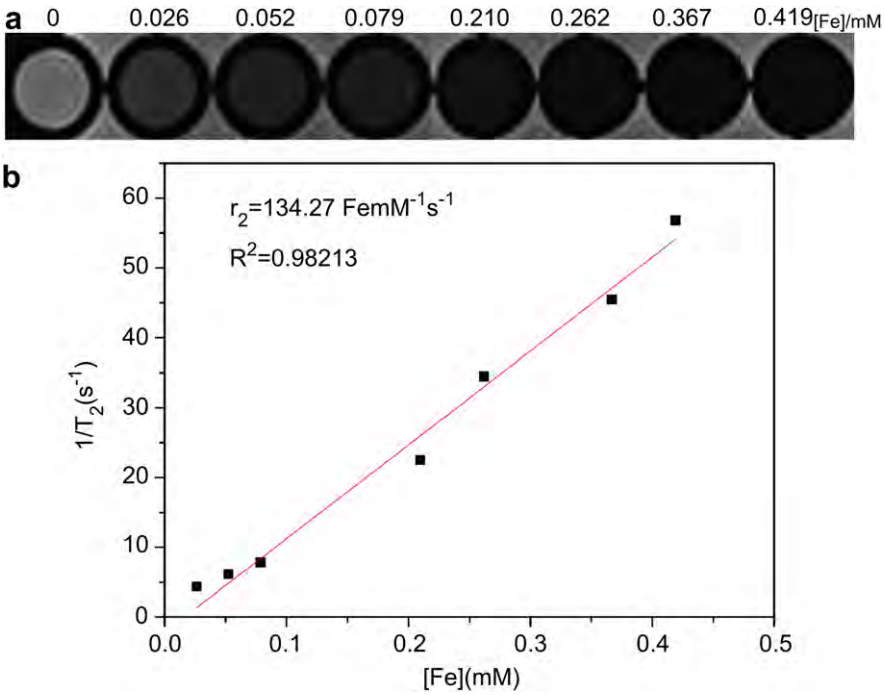

Fig. 12. (a) T_2-weight MR images of the aqueous solution containing magnetomicelles and different Fe concentrations; (b) T_2 relaxation rate (1/T2) as a function of Fe concentrations for the magnetomicelles.

3.4. Stability of magnetomicelles

The stability of the magnetomicelles is crucial to their use as drug carriers or MRI probes. Therefore, the size of the magnetomicelles is evaluated in an aqueous medium and media with different ionic strengths for 15 days. As shown in Fig. 9, the magnetomicelles remain well dispersed and the hydrodynamic diameter is virtually unchanged after 15 days. Furthermore, they exhibit good stability in a sodium chloride solution with high concentration. Our experiments disclose that the magnetomicelles are highly

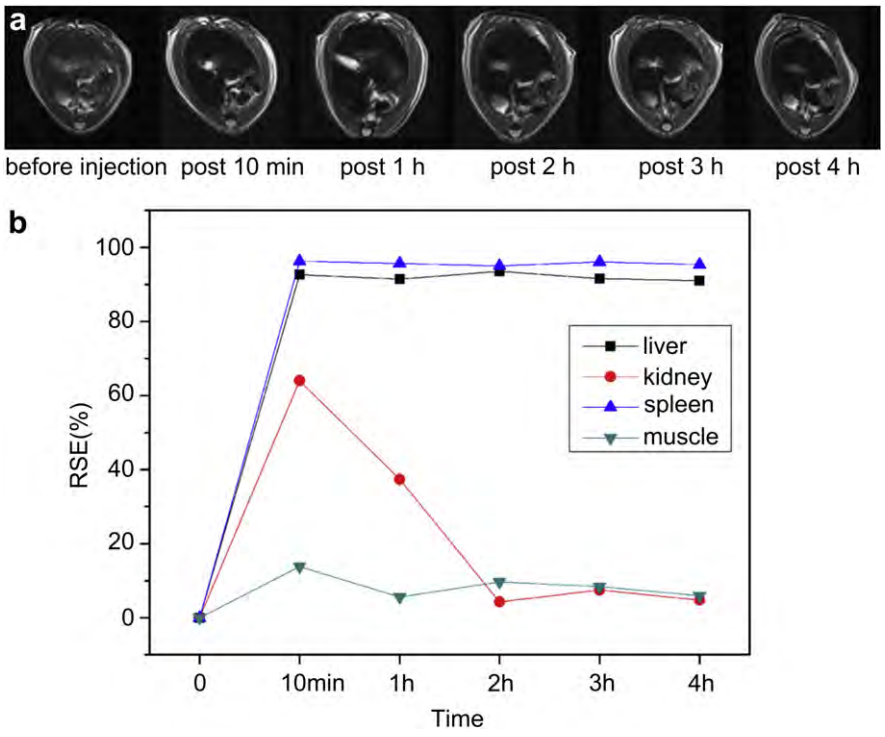

Fig. 13. (a) T_2-weighted images of mice at different time points before and after tail vein administration of magnetomicelles; (b) Relative signal enhancement values at the liver, kidney, spleen, and muscle before and after injection of magnetomicelles.

stable in in an aqueous medium even at a high chloride ion concentration.

3.5. In vitro cytotoxicity

To evaluate the cytocompatibity of the magnetomicelles, the cytotoxicity to HeLa cells is investigated using the MTT assay. Fig. 10 shows the HeLa cell viability after 24 h incubation in solutions with different concentrations of the magnetomicelles.A cell viability of over 80% is maintained as the magnetomicelle concentration is increased from 10 to 250 μg/mL, suggesting good compatibility and suitability as nanocarriers or probes in biomedical applications.

3.6. In vitro drug release studies

To evaluate the feasibility of magnetomicelles as nanocarriers in drug delivery, *in vitro* release of the hydrophobic drug, 5-FU, is studied under physiological conditions. 5-FU is chosen as the hydrophobic drug model because it is commonly administered in tumor therapy [42,43]. After the 5-FU is incorporated into the magnetomicelles, the drug loading content is calculated to be 20.94 wt % according to the method described in the experimental section. The *in vitro* drug release behavior of 5-FU from the magnetomicelles in PBS (pH = 7.4) at 37 °C is studied and shown in Fig. 11. The release of free 5-FU in PBS under the same conditions serves as the control experiment.The results reveals initial burst release from the 5-FU-loaded magnetomicelles (~30 wt% of the initial loaded amount) followed by sustained release (~30-83 wt% of the initial loaded amount). The initial burst release may be ascribed to the drug molecules located within the hydrophilic shell or at the interface between the micelle core and shell [32]. In contrast to the results obtained from the free release of 5-FU, the drug release rate from the magnetomicelles is impeded significantly. It is due to the hydrophobic–hydrophobic interactions between the hydrophobic drug molecules and hydrophobic segments of the magnetomicelles. The results demonstrate that magnetomicelles can be used as nanocarriers in drug delivery.

3.7. Relaxivity measurement and in vivo MRI

Iron oxide nanoparticles are known to shorten the transverse relaxation time of water protons and have been used as a negative contrast agent in MRI [44–46]. To evaluate the ability of magnetomicelles to enhance magnetic resonance imaging, the T_2-weighted MR images for different iron concentrations in an aqueous medium are acquired on a clinical 3T MRI instrument. As shown in Fig. 12a, sensitive and concentration-dependent dark areas can be observed from the MR images of the aqueous medium with the magnetomicelles. The reduced intensity is significant at high iron concentration showing that the magnetomicelles lead to an appreciable negative contrast enhancement (dark signal) in MRI.

The efficacy of an MRI negative contrast agent is commonly evaluated in terms of its transverse relaxivity rate, r_2 ($1/T_2$), which

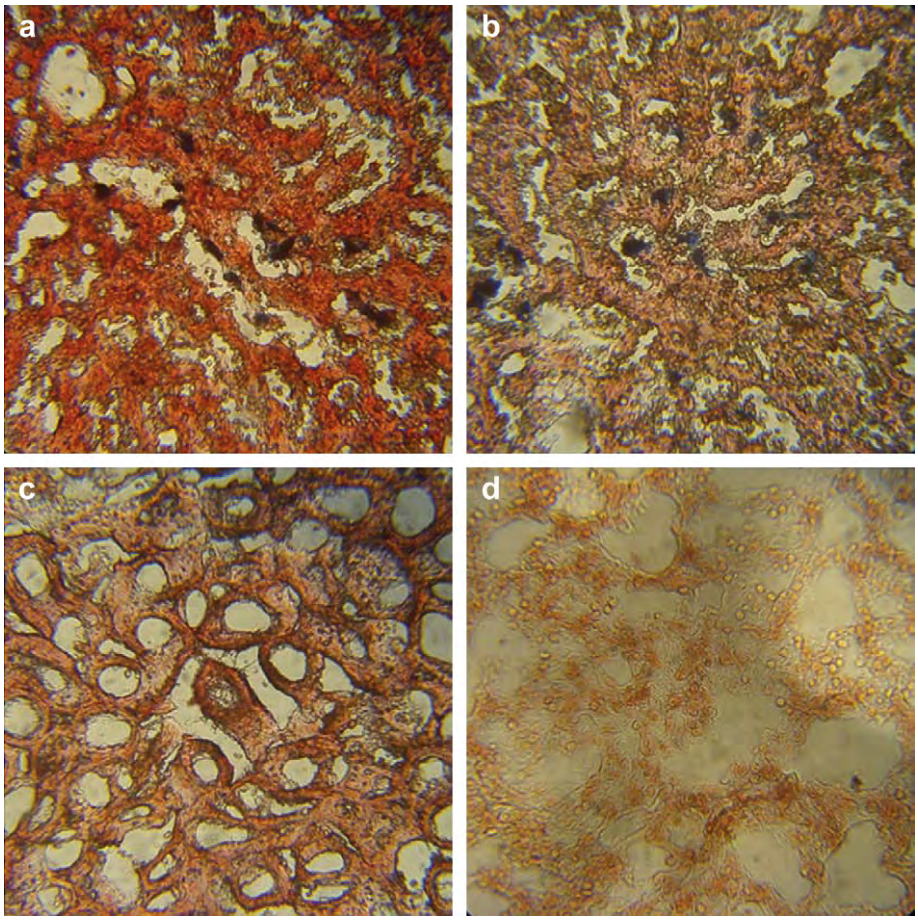

Fig. 14. Prussian blue stained images (×400) of (a) liver, (b) spleen, (c) kidney, and (d) lung after 8 h tail vein injection of magnetomicelles. (For interpretation of the references to colour in this figure legend, the reader is referred to the web version of this article.)

presents the efficiency of the magnetite nanoparticles to shorten the proton relaxation time.The relaxation rates of the magnetomicelles in Fig. 12b show that they vary linearly with iron concentrations according to the following relationship:

$$1/T_2 = 1/T_2^0 + r_2\left[\mathrm{Fe}\right], \quad (2)$$

where $1/T_2$.the observed relaxation rate in the presence of Fe_3O_4 nanoparticles, $1/T_2^0$. the relaxation rate of pure water, [Fe] is the concentration of the Fe_3O_4 nanoparticles, and r_2 is the transverse relaxivity. The r_2 relaxivity of the magnetomicelles is calculated to be 134.27 mM^{-1} s^{-1}, confirming that it is a good contrast agent in T_2-weighted MR images.

Generally, particulate MRI contrast agents derived from magnetic nanoparticles (e.g. commercially available Feridex and Resovit) always accumulate in the liver and spleen tissues thus facilitating the use of MRI to diagnose liver and spleen diseases.In order to evaluate the application of the magnetomicelles as *in vivo* MRI probes, female SD mice models are used. The *in vivo* MRI of a mouse liver using magnetomicelles as the contrast agent is depicted in Fig. 13a. The liver is darkened significantly after 10 min of magntetomicelles injection and a high contrast of liver tissue persists during observation for 4 h.The observation indicates that the magnetomicelles are effective T_2 MRI contrast agents in MR diagnostic imaging.

The signal intensity change in the organs during MRI shows the typical magnetic nanoparticle distribution, as reported previously on the administration of iron oxide nanoparticles containing PEGs [47].Hence, the time courses of the T_2 signal drops from the lung, liver, spleen, and kidney are recorded. As shown in Fig. 13b, significant contrast enhancements are observed from the liver and spleen immediately after 10 min of magnetomicelles injection and quantitative analysis reveals >90% SI change. The highest contrast enhancement of the liver and spleen lasts for 4 h without significant changes, corresponding to the highest magnetomicelle concentration in the liver and spleen. The high RSE value after 10 min post-injection and then the gradual decrease over a period of 2 h in the kidney suggest that the magnetomicelles can be excreted through the organ. Furthermore, no significant RSE change is observed from normal muscle confirming that the magnetomicelles cannot permeate normal tissues.It is highly possible that the magnetomicelles are captured by the macrophages of the RES in the liver and spleen.

To confirm the uptake of magnetomicelles by the liver and spleen tissues, the slides of different organs including the liver, spleen, kidney, and lung stained by Prussian blue are shown in Fig. 14. The blue color in the images indicates accumulation of the magnetite nanoparticles in the organs. As shown in Fig. 14a and b, some parts of the liver and spleen are stained blue and indicative of iron oxide. On the contrary, the images obtained from the lung and kidney show no significant Prussian blue staining (Fig. 14c and d).Hence, the magnetomicelles produce MRI contrast only in the liver and spleen.

4. Conclusion

A new type of magnetomicelles is prepared by the assembly of oleic acid modified Fe_3O_4 nanoparticles with fluorine-containing amphiphilic poly (HFMA-*g*-PEGMA) copolymer. The Fe_3O_4 clusters encapsulated by polymeric micelles are confirmed by TEM and these magnetomicelles are stable in both an aqueous solution as well as one with a high concentration of sodium chloride. The MTT cytotoxicity assay demonstrates that the magnetomicelles are cytocompatible. The potential applications of these magnetomicelles in drug delivery and *in vivo* MRI are demonstrated. The drug, 5-FU, incorporated into the magnetomicelles is controlled released into the PBS buffer. *In vitro* and *in vivo* MRI studies show that the magnetomicelles have high T_2 relaxivity (134.27 mM^{-1} s^{-1}) and good contrast effects in the liver and spleen. The results demonstrate that the magnetomicelles are potential nanocarriers in drug delivery and contrast agents in *in vivo* MRI.

Acknowledgments

We acknowledge joint financial support from the National Natural Science Foundation of China (No.50973027), Specialized Research Fund for the Doctoral Program of Higher Education (No.20094208110002), and Hong Kong Research Grants Council (RGC) General Research Funds (GRF) No. CityU 112510.

References

[1] Durán JDG, Arias JL, Gallardo V, Delgado AV. Magnetic colloids as drug vehicles. J Pharm Sci 2008;97:2948–83.
[2] Purushotham S, Ramanujan RV. Thermoresponsive magnetic composite nanomaterials for multimodal cancer therapy. Acta Biomater 2010;6:502–10.
[3] Zhang J, Misra RDK. Magnetic drug-targeting carrier encapsulated with thermosensitive smart polymer: core-shell nanoparticle carrier and drug release response. Acta Biomater 2007;3:838–50.
[4] Takahashi M, Akiyama Y, Ikezumi J, Nagata T, Yoshino T, Iizuka A, et al. Magnetic separation of melanoma-specific cytotoxic t lymphocytes from a vaccinated melanoma patient's blood using MHC/peptide complex-conjugated bacterial magnetic particles. Bioconjug Chem 2009;20:304–9.
[5] Gai Q-Q, Qu F, Liu Z-J, Dai R-J, Zhang Y-K. Superparamagnetic lysozyme surface-imprinted polymer prepared by atom transfer radical polymerization and its application for protein separation. J Chromatogr A 2010;1217:5035–42.
[6] Zhang L, Xue H, Gao C, Carr L, Wang J, Chu B, et al. Imaging and cell targeting characteristics of magnetic nanoparticles modified by a functionalizable zwitterionic polymer with adhesive 3,4-dihydroxyphenyl-l-alanine linkages. Biomaterials 2010;31:6582–8.
[7] Hong RY, Feng B, Chen LL, Liu GH, Li HZ, Zheng Y, et al. Synthesis, characterization and MRI application of dextran-coated Fe_3O_4 magnetic nanoparticles. Biochem Eng J 2008;42:290–300.
[8] Kluchova K, Zboril R, Tucek J, Pecova M, Zajoncova L, Safarik I, et al. Superparamagnetic maghemite nanoparticles from solid-state synthesis – their functionalization towards peroral MRI contrast agent and magnetic carrier for trypsin immobilization. Biomaterials 2009;30:2855–63.
[9] Bagaria HG, Ada ET, Shamsuzzoha M, Nikles DE, Johnson DT. Understanding mercapto ligand exchange on the surface of FePt nanoparticles. Langmuir 2006;22:7732–7.
[10] Shultz MD, Reveles JU, Khanna SN, Carpenter EE. Reactive nature of dopamine as a surface functionalization agent in iron oxide nanoparticles. J Am Chem Soc 2007;129:2482–7.
[11] Zhang M, Cheng D, He X, Chen L, Zhang Y. Magnetic silica-coated submicrospheres with immobilized metal ions for the selective removal of bovine hemoglobin from bovine blood. Chem Asian J 2010;5:1332–40.
[12] Qiu P, Jensen C, Charity N, Towner R, Mao C. Oil phase evaporation-induced self-assembly of hydrophobic nanoparticles into spherical clusters with controlled surface chemistry in an oil-in-water dispersion and comparison of behaviors of individual and clustered iron oxide nanoparticles. J Am Chem Soc 2010;132:17724–32.
[13] Pan X, Guan J, Yoo J-W, Epstein AJ, Lee LJ, Lee RJ. Cationic lipid-coated magnetic nanoparticles associated with transferrin for gene delivery. Int J Pharm 2008;358:263–70.
[14] Yang H, Zhang J, Tian Q, Hu H, Fang Y, Wu H, et al. One-pot synthesis of amphiphilic superparamagnetic fept nanoparticles and magnetic resonance imaging in vitro. J Magn Magn Mater 2010;322:973–7.
[15] Lu J, Ma S, Sun J, Xia C, Liu C, Wang Z, et al. Manganese ferrite nanoparticle micellar nanocomposites as MRI contrast agent for liver imaging. Biomaterials 2009;30:2919–28.
[16] Kaiser A, Dutz S, Schmidt AM. Kinetic studies of surface-initiated atom transfer radical polymerization in the synthesis of magnetic fluids. J Polym Sci Part A Polym Chem 2009;47:7012–20.
[17] Zhang L, Eisenberg A. Multiple morphologies and characteristics of "crew-cut" micelle-like aggregates of polystyrene-b-poly(acrylic acid) diblock copolymers in aqueous solutions. J Am Chem Soc 1996;118:3168–81.
[18] Lodge TP, Pudil B, Hanley KJ. The full phase behavior for block copolymers in solvents of varying selectivity. Macromolecules 2002;35:4707–17.
[19] Wan S, Jiang M, Zhang G. Dual temperature- and pH-dependent self-assembly of cellulose-based copolymer with a pair of complementary grafts. Macromolecules 2007;40:5552–8.

[20] Zhang X, Shen Z, Feng C, Yang D, Li Y, Hu J, et al. PMHDO-g-PEG double-bond-based amphiphilic graft copolymer: synthesis and diverse self-assembled nanostructures. Macromolecules 2009;42:4249–56.
[21] Tsai H-C, Chang W-H, Lo C-L, Tsai C-H, Chang C-H, Ou T-W, et al. Graft and diblock copolymer multifunctional micelles for cancer chemotherapy and imaging. Biomaterials 2010;31:2293–301.
[22] Liggins RT, Burt HM. Polyether-polyester diblock copolymers for the preparation of paclitaxel loaded polymeric micelle formulations. Adv Drug Deliv Rev 2002;54:191–202.
[23] Ai H, Flask C, Weinberg B, Shuai XT, Pagel MD, Farrell D, et al. Magnetite-loaded polymeric micelles as ultrasensitive magnetic-resonance probes. Adv Mater 2005;17:1949–52.
[24] Yang J, Lee T-I, Lee J, Lim E-K, Hyung W, Lee C-H, et al. Synthesis of ultrasensitive magnetic resonance contrast agents for cancer imaging using PEG-fatty acid. Chem Mater 2007;19:3870–6.
[25] Wang W-C, Neoh K-G, Kang E-T. Surface functionalization of Fe_3O_4 magnetic nanoparticles via raft-mediated graft polymerization. Macromol Rapid Commun 2006;27:1665–9.
[26] Hickey RJ, Haynes AS, Kikkawa JM, Park S-J. Controlling the self-assembly structure of magnetic nanoparticles and amphiphilic block-copolymers: from micelles to vesicles. J Am Chem Soc 2011;133:1517–25.
[27] Bai Y, Teng B, Chen S, Chang Y, Li Z. Preparation of magnetite nanoparticles coated with an amphiphilic block copolymer: a potential drug carrier with a core-shell-corona structure for hydrophobic drug delivery. Macromol Rapid Commun 2006;27:2107–12.
[28] Yang R, Wang Y, Zhou D. Novel hydroxyethylcellulose-graft-poly acrylamide copolymer for separation of double-stranded DNA fragments by CE. Electrophoresis 2007;28:3223–31.
[29] Zhang J, Wang Y, Liang D, Ying Q, Chu B. Association behavior of pdma-g-pmma in mixed solvents and its application as a DNA separation medium. Macromolecules 2005;38:1936–43.
[30] Wan S, Huang J, Yan H, Liu K. Size-controlled preparation of magnetite nanoparticles in the presence of graft copolymers. J Mater Chem 2006;16:298–303.
[31] Yuan W, Yuan J, Zhou L, Wu S, Hong X. Fe_3O_4@poly(2-hydroxyethyl methacrylate)-graft-poly([var epsilon]-caprolactone) magnetic nanoparticles with branched brush polymeric shell. Polymer 2010;51:2540–7.
[32] Allen C, Maysinger D, Eisenberg A. Nano-engineering block copolymer aggregates for drug delivery. Colloids Surf B 1999;16:3–27.
[33] Krafft MP. Fluorocarbons and fluorinated amphiphiles in drug delivery and biomedical research. Adv Drug Deliv Rev 2001;47:209–28.
[34] Hussain H, Busse K, Kressler J. Poly(ethylene oxide)- and poly(perfluorohexylethyl methacrylate)-containing amphiphilic block copolymers: association properties in aqueous solution. Macromol Chem Phys 2003;204:936–46.
[35] Lodge TP, Rasdal A, Li Z, Hillmyer MA. Simultaneous, segregated storage of two agents in a multicompartment micelle. J Am Chem Soc 2005;127:17608–9.
[36] Cha MS, Kim JW, Ha J-W, Park IJ, Lee S-B, Yang T, et al. Self-emulsification and surface modification effect of fluorinated amphiphilic acrylate graft copolymers. J Polym Sci Part A Polym Chem 2010;48:4574–82.
[37] Xiong S-D, Li L, Wu S-L, Xu Z-S, Chu PK. Synthesis and properties of fluorine-containing amphiphilic graft copolymer p(HFMA)-g-P(SPEG). J Polym Sci Part A Polym Chem 2009;47:4895–907.
[38] Xiong S-D, Li L, Jiang J, Tong L-P, Wu S, Xu Z-S, et al. Cationic fluorine-containing amphiphilic graft copolymers as DNA carriers. Biomaterials 2010;31:2673–85.
[39] Sauzedde F, Elaïssari A, Pichot C. Hydrophilic magnetic polymer latexes. 1. Adsorption of magnetic iron oxide nanoparticles onto various cationic latexes. Colloid Polym Sci 1999;277:846–55.
[40] Nakamura K, Endo R, Takeda M. Surface properties of styrene-ethylene oxide block copolymers. J Polym Sci 1976;14:1287–95.
[41] Kim B-S, Taton TA. Multicomponent nanoparticles via self-assembly with cross-linked block copolymer surfactants. Langmuir 2006;23:2198–202.
[42] Prabaharan M, Grailer JJ, Pilla S, Steeber DA, Gong S. Amphiphilic multi-arm block copolymer based on hyperbranched polyester, poly(l-lactide) and poly(ethylene glycol) as a drug delivery carrier. Macromol Biosci 2009;9:515–24.
[43] Sivakumar S, Bansal V, Cortez C, Chong S-F, Zelikin AN, Caruso F. Degradable, surfactant-free, monodisperse polymer-encapsulated emulsions as anticancer drug carriers. Adv Mater 2009;21:1820–4.
[44] Jun Y-W, Seo J-W, Cheon J. Nanoscaling laws of magnetic nanoparticles and their applicabilities in biomedical sciences. Acc Chem Res 2008;41:179–89.
[45] Sun S. Recent advances in chemical synthesis, self-assembly, and applications of fept nanoparticles. Adv Mater 2006;18:393–404.
[46] Maeng JH, Lee D-H, Jung KH, Bae Y-H, Park I-S, Jeong S, et al. Multifunctional doxorubicin loaded superparamagnetic iron oxide nanoparticles for chemotherapy and magnetic resonance imaging in liver cancer. Biomaterials 2010;31:4995–5006.
[47] Park J, Yu MK, Jeong YY, Kim JW, Lee K, Phan VN, et al. Antibiofouling amphiphilic polymer-coated superparamagnetic iron oxide nanoparticles: synthesis, characterization, and use in cancer imaging in vivo. J Mater Chem 2009;19:6412–7.